Desalination and Water Treatment
www.deswater.com
doi: 10.5004/dwt.2023.29326

286 (2023) 183–191
February

Cross-linked sodium alginate-carboxymethyl chitosan hydrogel beads for adsorption of Ni(II) ions

Qingping Song, Bangjie Ouyang, Ying Lin, Chongxia Wang*

School of Chemical and Environmental Engineering, Anhui Polytechnic University, Anhui, China, emails: wangcx@ahpu.edu.cn (C. Wang), songqp@ahpu.edu.cn (Q. Song), 210619475@qq.com (B. Ouyang), ly2005501@163.com (Y. Lin)

Received 1 August 2022; Accepted 19 January 2023

ABSTRACT

A cross-linked sodium alginate-carboxymethyl chitosan hydrogel beads (CHB) was synthesized using calcium chloride and epichlorohydrin as cross-linkers. The synthesized CHB adsorbent was characterized by Fourier-transform infrared spectroscopy (FTIR), scanning electron microscopy and energy-dispersive X-ray spectroscopy. The Ni(II) removal by the CHB was investigated, several parameters influencing the adsorption of Ni(II) ions such as contact time, pH, initial Ni(II) concentration and regeneration performance were investigated. Results revealed that the adsorption equilibrium was reached within 6 h and the maximum capacity of CHB for Ni(II) was obtained to be 128.4 mg/g. The equilibrium adsorption data fitted well to the Freundlich model and the adsorption kinetic data followed the pseudo-second-order model. Furthermore, the prepared CHB showed good adsorption performance after five cycles of regeneration. Finally, FTIR and X-ray photoelectron spectroscopy analysis showed that the hydroxyl, amino and carboxyl groups were involved in the adsorption of Ni(II).

Keywords: Adsorption; Carboxymethyl chitosan; Cross-linking; Hydrogel; Sodium alginate

1. Introduction

Water pollution by heavy metals is becoming a severe global issue due to toxicity, non-degradability and accumulation nature of heavy metals through a food chain. Ni(II) is often detected in industrial wastewaters, which originate from silver refineries, zinc base casting, electroplating, and storage battery industries [1]. The main methods for removing Ni(II) from an aqueous environment include ion exchange, chemical precipitation, electrochemical reduction, membrane separation and adsorption [2,3], among which, adsorption has been found to be the best technology due to its high efficiency, low operating cost, eco-friendly and without secondary pollution [4,5].

In recent years, biosorption is a promising technology for the removal of heavy metal ions from solution. Bioadsorbents have gained considerable attention due to their low cost, their nontoxic, biodegradable and natural availability [6,7]. For example, chitosan, sodium alginate, starch, and cellulose, have been used for heavy metal removal [8,9]. Among these adsorbents, sodium alginate (SA), a polysaccharide extracted from brown algae, is considered to be the most promising candidate a natural polysaccharide biopolymer. It is composed of chains of 1,4-linked β-D-mannuronic (M) blocks and α-L-guluronic (G) blocks. sodium alginate contains abundance of hydroxyl and carboxyl groups along its structure that have strong affinity towards heavy metals. Nevertheless, sodium alginate tends to dissolve in water, which limits its application in adsorption. A common technique that has been used to overcome this problem is by turning sodium alginate into hydrogel [10]. Calcium ion is the most commonly used cation to prepare alginate hydrogel. In

* Corresponding author.

the presence of calcium ion, sodium alginate is synthesized into insoluble calcium alginate with "egg-box" macromolecular structure [11].

Similarly, a carboxymethyl chitosan (CMC), a water–soluble derivative of chitosan, contains amino, hydroxyl and carboxyl groups, which is regarded as a prospective adsorbent for adsorption of heavy metal [12]. Nevertheless, it couldn't be used for the recovery of heavy ions because of being water dissolvable and having weak chemical stability [13]. In order to overcome these limitations, chemical modification with a cross-linking agent or physical blending with other biopolymers can be regarded as one of the best techniques [14–16]. Polymer blends refer to the physical mixing of two or more polymers to incorporate their best properties, enhanced mechanical characteristics and effective removal of heavy metal ions from wastewater [17–19]. However, carboxyl groups in SA/CMC hydrogel will be occupied in ionic cross-linking reaction, which would lead to a decrease in active sites for heavy metal ion uptake. Also, the hydrogels via purely ionic cross-linking have a limitation in that cross-linking stability decrease especially in acidic medium due to exchanging of calcium ions with hydrogen ions [20]. Therefore, developing novel strategies to design and construct powerful alginate-based adsorbents are desirable.

The present study aimed to construct a novel hydrogel adsorbent with better adsorption performance and acid resistance ability. Ionic coacervation and chemical cross-linking process was used to prepare cross-linked sodium alginate-carboxymethyl chitosan hydrogel beads (CHB). Calcium chloride and epichlorohydrin were used as a physical and chemical cross-linker, respectively. First, mixed solution of sodium alginate and carboxymethyl chitosan was dropped into calcium chloride solution to form blend hydrogel beads by ionic cross-linking method. Then, the obtained beads were further cross-linked with epichlorohydrin. In order to release more adsorption sites, the prepared cross-linked beads were further treated with strong acid to remove calcium ions. Finally, the CHB adsorbent was obtained and characterized by Fourier-transform infrared spectroscopy (FTIR), scanning electron microscopy (SEM) and energy-dispersive X-ray spectroscopy (EDS) spectrometer to identify the structures, morphology and elemental analysis. Unlike traditional powder or bulk adsorbents, the CHB are easily separated and regenerated in acid solution because of the form of a three-dimensional network structure in cross-linking reaction, which is benefit for industrial wastewater treatment. The adsorbent was used for adsorption of Ni(II) from aqueous solutions. The pH value, adsorption time, initial Ni(II) concentration and reusability were investigated in the experiment. The adsorption mechanism was explored by FTIR and X-ray photoelectron spectroscopy (XPS) characterizations.

2. Experimental set-up

2.1. Materials

Sodium alginate (SA, Mv = 4.3×10^5) and chitosan (93% deacetylated, Mv = 6.2×10^5) were purchased from Sinopharm Chemical Reagent (Shanghai, China). $Ni(NO_3)_2\cdot6H_2O$, KOH, HCl, $CaCl_2$, EtOH, epichlorohydrin and all other reagents were obtained from Sinopharm Chemical Reagent (Shanghai, China) as analytical grade. All the solutions were prepared with distilled water.

2.2. Synthesis of adsorbents

Carboxymethyl chitosan (CMC) was prepared according to the previous literature [21]. Cross-linked sodium alginate-carboxymethyl chitosan hydrogel beads (CHB) was prepared as follows. First, 2.0 g sodium alginate was dissolved in 98 mL water until a clear solution was obtained. Meanwhile, 2.0 g CMC was dissolved in 48 mL distilled water. Next, the above two solutions were mixed together for 3 h by strong magnetic stirring. After that, the mixed solution was added dropwise to a 200 mL $CaCl_2$ solution (5%, w/v) through a 16 G syringe needle to form beads, which were gently stirred in the aforementioned solution and solidified for 1 h. Then, the beads were filtered and washed several timed with water. The prepared beads were cross-linked with epichlorohydrin (4 mL) in 100 mL ethanol solvent containing 0.1 M potassium hydroxide.

After reaction 3 h at 50°C, the cross-linked beads were filtered, and added into 0.2 M HCl solution for 24 h to removal calcium ion. Afterwards, the acid-washed beads were filtered and immersed in 0.1 M NaOH solution for 0.5 h to activated carboxyl group. Finally, the beads were washed with water several times, and then freeze-dried for 24 h to obtain CHB adsorbent. The preparation process is illustrated in Fig. 1.

2.3. Characterization of CHB

FTIR spectra of the samples were measured using a Fourier transform infrared spectrometer, Model EQUINOX55 (Bruke). The surface morphology of the CHB adsorbent was examined by using a scanning electron microscope (Hitachi S-4800) coupled with EDS spectrometer. X-ray photoelectron spectra of CHB adsorbents before and after Ni(II) adsorption were obtained by using an ESCALAB 250 XPS spectrometer (Thermo-VG Scientific).

2.4. Batch Ni(II) removal experiments

Batch adsorption experiments were carried out to evaluate adsorption capacities of CHB and all adsorption experiments were carried out at 25°C. $Ni(NO_3)_2\cdot6H_2O$ was used as sources of Ni(II). Typically, 50 mg of CHB were added into a 50 mL solution of known Ni(II) concentrations and stirred at the fixed speed (150 rpm) with thermostatic stirrer. The initial pH value was adjusted by 0.1 M HCl or 0.1 M NaOH solutions by using a Model PHS-25 pH-meter (Shanghai Leici, China). At given time, the CHB was filtrated from the solutions and the concentration of Ni(II) remaining in the solution was determined by atomic absorption spectrophotometer (TAS900, Beijing Purkinje). The adsorption capacity (q) was calculated according to the following equation:

$$q = \frac{V\left(C_i - C_f\right)}{m} \tag{1}$$

where q is the metal adsorption capacity (mg/g), C_i is the initial concentration of Ni(II) (mg/L), C_f is the final

concentration of Ni(II) (mg/L), V is the volume of the solution (L), and m is the weight of CHB added into the flask.

To determine the kinetics performances, 50 mg of CHB was added to 50 mL of Ni(II) solution (200 or 300 mg/L). The mixture was then stirred, and samples were filtered at different time intervals and analyzed the filtrate solution. Equilibrium adsorption isotherm experiments were conducted over a range of initial Ni(II) concentrations from 100–300 mg/L. 50 mg of CHB was added into 50 mL of the solutions. The mixtures were stirred at 25°C for 6 h. After adsorption, the solution was filtered and the final concentration of Ni(II) was determined.

2.5. Regeneration experiment

In the regeneration experiment, 50 mg of adsorbent was loaded with 50 mL of 300 mg/L Ni(II) solution. Ni(II) loaded adsorbents was collected. The adsorbents were added into 50 mL of 0.1 M HCl solutions for 2 h at room temperature to ensure the desorption of Ni(II) from the adsorbent. To use adsorbent in next cycle, the adsorbent was washed several times with water. Then, the treated CHB was applied in the recycled adsorption study. The adsorption/desorption measurements were repeated five times.

3. Results and discussions

3.1. Characterization of the CHB

FTIR spectra of sodium alginate (SA), carboxymethyl chitosan (CMC) and CHB before and after Ni(II) adsorption are shown in Fig. 2. In the spectrum of SA, the major bands can be assigned as follows: 3,418 cm^{-1} (–OH stretching vibration), 2,929 cm^{-1} (–CH stretching vibration), 1,610 cm^{-1} ($–COO^-$ asymmetric stretching), 1,418 cm^{-1} ($–COO^-$ symmetric stretching), 1,030 cm^{-1} (C–OH stretching vibration) [22,23]. In the spectrum of CMC, the broad characteristic peak appeared at 3,423 cm^{-1} relating to the stretching –OH and $–NH_2$ groups. The peaks at 1,599 and 1,415 cm^{-1} were attributed to the asymmetric stretching and symmetric stretching of $–COO^-$ groups, respectively [24–26]. Compared with the spectra of SA and CMC, the wide peak at 3,263 cm^{-1} of CHB corresponding to the stretching vibration of $–NH_2$ and –OH groups shifted to lower frequency. It indicated the $–NH_2$ and –OH groups of adsorbents were cross-linked with *epichlorohydrin*. The two strong bands at 1,588 and 1,404 cm^{-1} assigned to asymmetric and symmetric stretching of $–COO^-$ groups also shifted to lower wavenumbers, respectively. All of these results confirmed that the blending between SA and CMC was successful.

The morphology of CHB adsorbent was assessed through scanning electron microscopy (SEM). As it is depicted in Fig. 3, the beads have a spherical shape and the diameter of the hydrogel beads mainly ranges from 2.0 to 3.0 mm. In addition, the beads showed a rough surface. The results of SEM showed a good compatibility between SA and CMC.

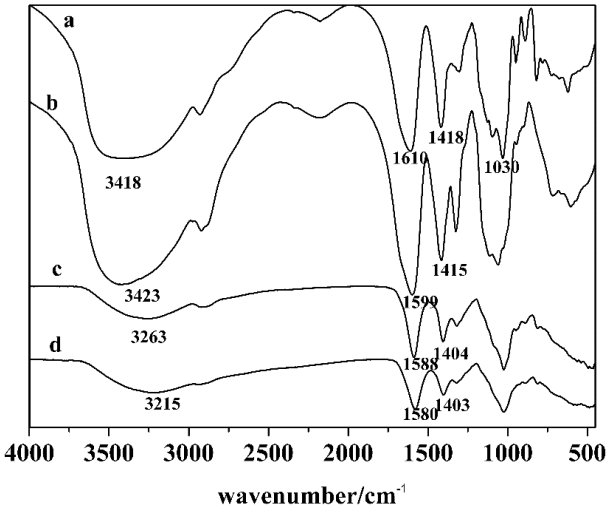

Fig. 2. FTIR spectra of SA (a), CMC (b) and CHB before (c) and after Ni(II) adsorption (d).

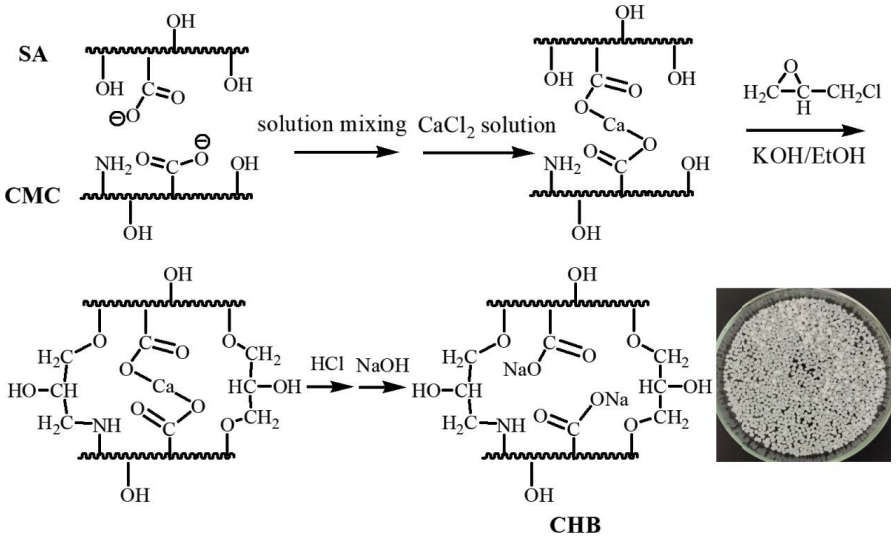

Fig. 1. Preparation scheme of CHB adsorbent.

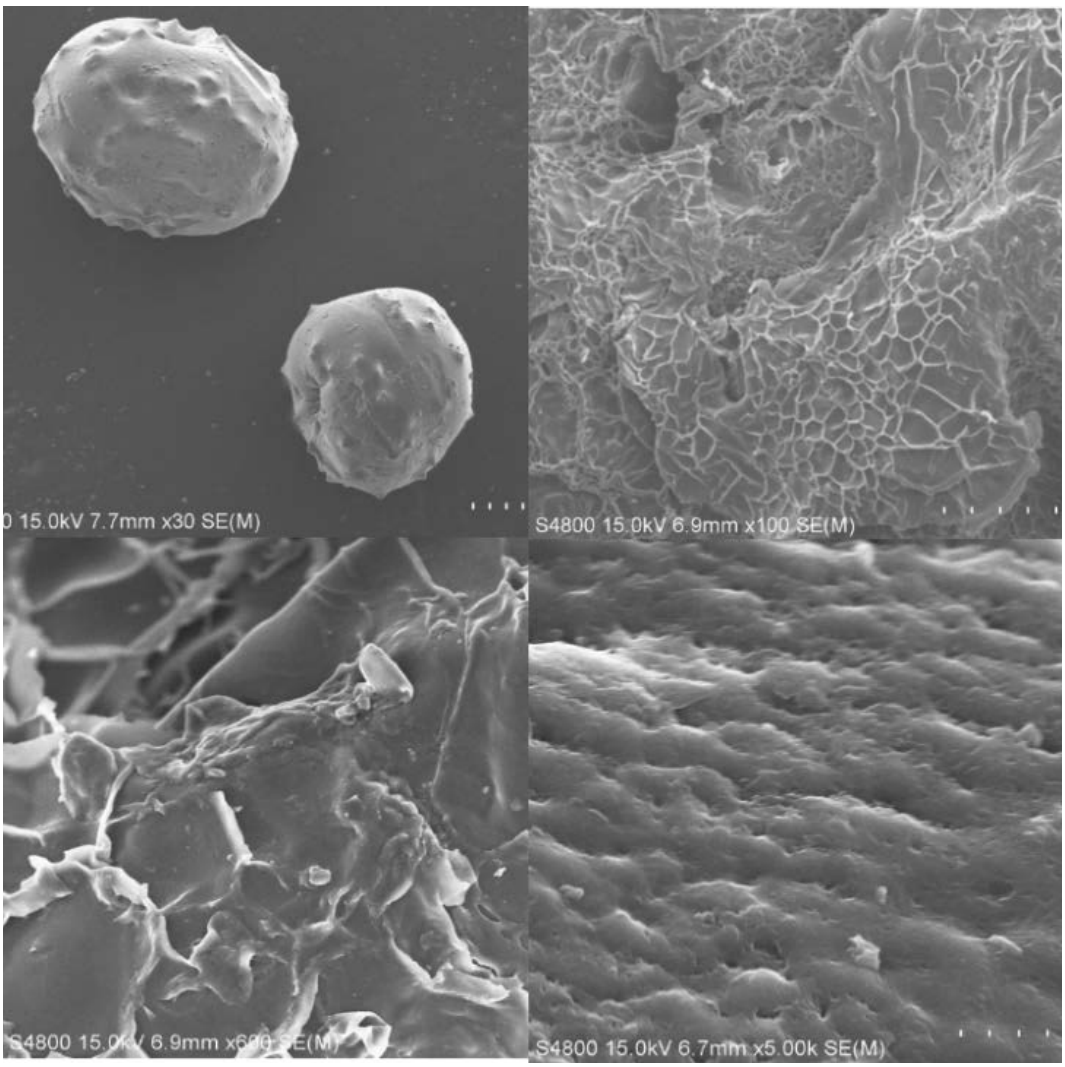

Fig. 3. SEM images of the CHB adsorbent.

To verify the decalcification reaction of CHB, the EDS of the CHB and undecalcified CHB were used to perform elemental analysis of the adsorbent, and the results were shown in Fig. 4. It can be seen clearly from EDS analysis, C, O, N, Ca and Na were present in the beads. The N element was obtained from the OCMC, which confirmed a successful synthesis of blended gel beads. However, in the undecalcified CHB, the percentage of Ca was 4.89%. After 24 h of decalcification reaction with 0.2M HCl, the percentage of Ca in CHB decreased significantly to 0.08%, indicating the method of decalcification was effective. In addition, the percentage of Na increased from 0.53% to 11.34%, which indicated Ca^{2+} was almost exchanged by Na^{+} on acid–base neutralization.

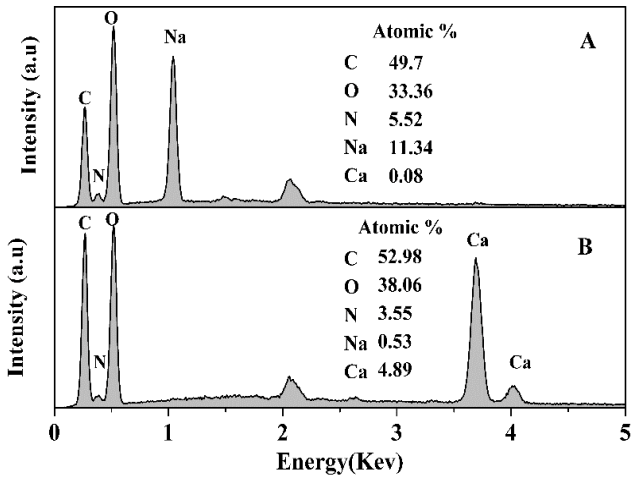

Fig. 4. EDS results of the CHB adsorbent (A) and undecalcified CHB (B).

3.2. Effect of pH

To study the effect of pH on the adsorption process with the CHB, experiments were conducted in the pH range 1.0–7.0 and the result is shown in Fig. 5. Within the

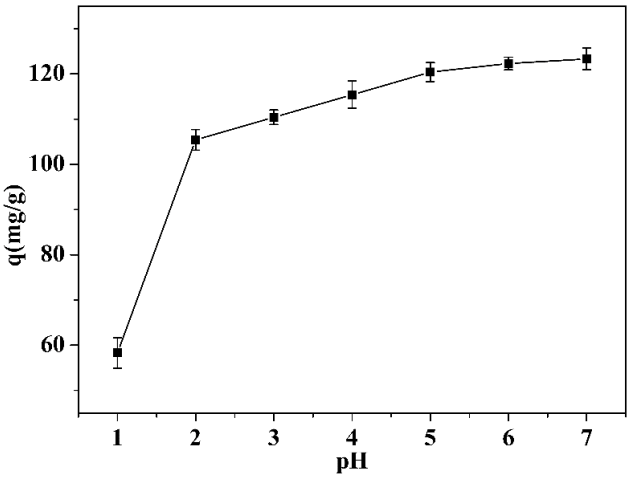

Fig. 5. Effect of pH toward the removal of Ni(II) using CHB (Ni(II): 200 mg/L; dosage: 1.0 g/L; contact time: 6 h; temperature: 25°C).

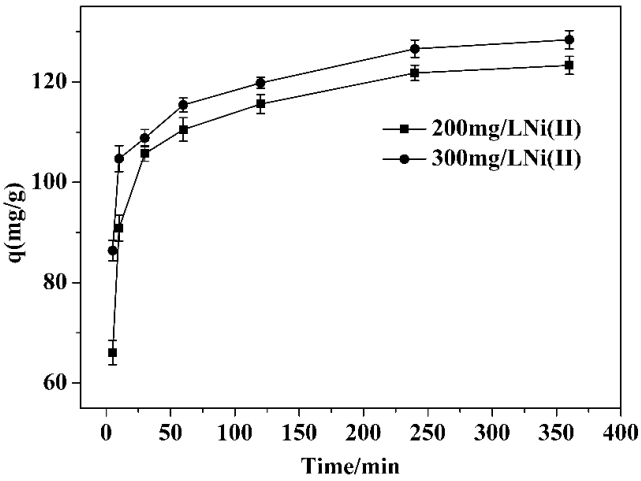

Fig. 6. Kinetic adsorption results of Ni(II) on CHB (pH: 7.0; dosage: 1.0 g/L; temperature: 25°C).

range of pH values varied from 1.0 to 2.0, the adsorption capacity significantly increased from 58.3 to 105.4 mg/g. With further increase of pH (2.0–7.0), the adsorption capacity of Ni(II) gradually reached the maximum of 123.3 mg/g at pH 7.0. With a pH greater than 7.0, precipitation occurred between Ni(II) ions and hydroxide ions. Therefore, pH 7.0 was selected as the optimal value for Ni(II) adsorption on the CHB.

At lower pH value, the amino groups ($–NH_2$) on CHB surfaces were more easily protonated ($–NH_3^+$), inducing an electrostatic repulsion between Ni(II) and positively charged surface of adsorbents. As pH increased, the reducing protonation of the amino groups and the increasing the number of carboxylate groups ($–COO^-$) could improve the adsorption owing to electrostatic binding between Ni(II) and negatively charged active sites [27,28].

3.3. Effect of contact time and kinetic modeling

The adsorption rate related with the contact time is one of the important characteristics. The effect of contact time on the adsorption of CHB for Ni(II) was investigated at different initial solute concentrations and the results are shown in Fig. 6. It was found that the absorbed amount of Ni(II) increased with increasing Ni(II) concentration from 200 to 300 mg/L. This might be because, at higher concentrations, the driving force for ion migration between the aqueous phase and solid phase enhanced [29]. In addition, the rates of adsorption of Ni(II) on CHB were seen to increase markedly during the first 60 min and gradually approach the limiting adsorption (128.4 mg/g) after 240 min (6 h). The explanation may be that a large number of free adsorption sites on the surface were void and that Ni(II) easily interacted with these sites during the initial stage. With time increasing, the remaining vacant sites are not easily occupied due to the reduction of the adsorption sites [13]. Then adsorption rate slows down and gradually reaches to the equilibrium.

In order to investigate the adsorption mechanisms, the adsorption experimental data were fitted using the linear form of pseudo-first-order [Eq. (2)] and the pseudo-second-order equations [Eq. (3)] [30].

$$\log\left(q_e - q_t\right) = \log q_e - \frac{k_1}{2.303}t \tag{2}$$

$$\frac{t}{q_t} = \frac{1}{k_2 q_e^2} + \frac{t}{q_e} \tag{3}$$

where q_e and q_t (mg/g) are the adsorption capacities of Ni(II) ions adsorbed onto CHB at equilibrium and at time t, respectively. k_1 (min^{-1}) and k_2 (g/mg·min) are adsorption rate constants of the pseudo-first-order and pseudo-second-order, respectively.

Then the two kinetic models have been applied to fit the experimental data, respectively. The linear fitting results are shown in Fig. 7 and their parameters are all listed in Table 1. On the basis of the correlation coefficients (R^2), the adsorption behaviors of Ni(II) on CHB fitted well with the pseudo-second-order kinetic model. The calculated q_e values were in agreement with the theoretical ones. Therefore, the adsorption kinetics follows the pseudo-second-order model, suggesting that chemisorption is the dominant rate-limiting step [31].

3.4. Desorption and regeneration analysis

Recycle studies were performed to explore the sustainability and cost effectiveness of the CHB. Most adsorbents are in the form of powder to increase the contact area of the adsorbent and the solution, which clearly leads to the difficulty of collecting the adsorbent after sorption [32]. In contrast, CHB beads can be easily desorbed the metals under acid conditions and collected after adsorption.

In the desorption experiment, five adsorption–desorption cycles were conducted, and the 0.1M HCl solution was employed as the desorption agent to desorb Ni(II) from CHB adsorbents. The corresponding adsorption capacities are shown in Fig. 8. The adsorption capacity of Ni(II)

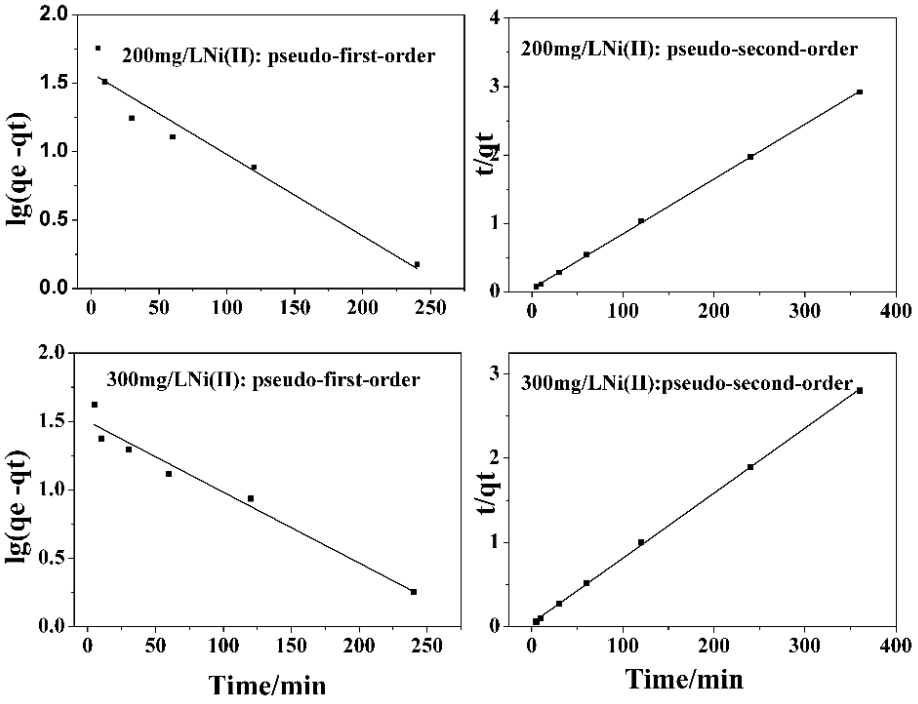

Fig. 7. Kinetic modeling of Ni(II) adsorption by CHB (pH: 7.0; dosage: 1.0 g/L; temperature: 25°C).

Table 1
Parameters of kinetic models of Ni(II) adsorption onto CHB

		Ion concentration (mg/L)	
Kinetic model	Model parameter	200 mg/L	300 mg/L
Pseudo-first-order model	$q_{e,\exp}$ (mg/g)	123.3	128.4
	$q_{e,\mathrm{cal}}$ (mg/g)	37.6	31.6
	k_1 (min^{-1})	0.0137	0.0119
	R^2	0.932	0.956
Pseudo-second-order model	k_2 (10^3 g/mg·min)	1.355	1.484
	$q_{e,\mathrm{cal}}$ (mg/g)	124.8	129.5
	R^2	0.999	0.999

on CHB decreased slowly with increasing cycle numbers in the five cycles, and at the end of five regeneration cycles, the sorption capacity maintained at 70.3% of the initial value. The results indicated that CHB has a great potential in the practical adsorption for metal ions.

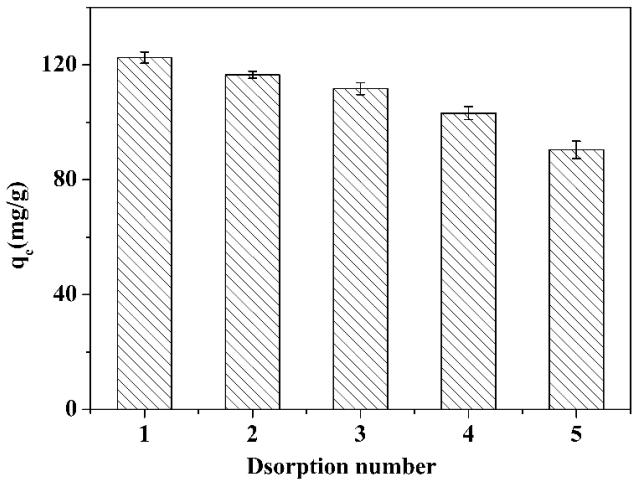

Fig. 8. Adsorption capacity of CHB adsorbent for Ni(II) during cyclic experiments (initial concentration: 300 mg/L; dosage: 1.0 g/L; at pH 7.0; desorption time: 120 min; temperature: 25°C).

3.5. Adsorption isotherms

The adsorption isotherm model describes the interaction of adsorbate with adsorbents and is important for predicting adsorption performance of the adsorbent. Two of the most commonly used isotherm theories have been adopted in this work, namely Langmuir and Freundlich [33]. The Langmuir isotherm model is assumed to have affinity for monolayer adsorption. Whereas the Freundlich isotherm adsorption model considered that multilayer adsorption occurs on heterogeneous surfaces [34]. The form of the Langmuir isotherm and Freundlich are given as follows:

Langmuir isotherm model: $$q_e = \frac{q_m K_L C_e}{1 + K_L C_e} \quad (4)$$

Freundlich isotherm model: $$q_e = K_F C_e^{1/n} \quad (5)$$

where C_e (mg/L) is the equilibrium concentration of residual ions in the solution and q_m is the maximum amount of

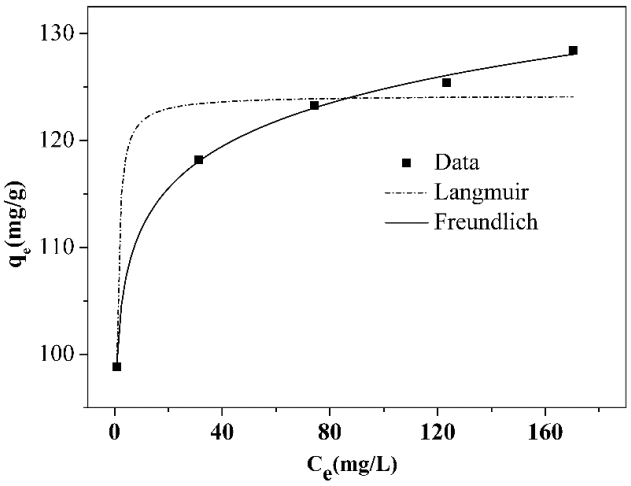

Fig. 9. Adsorption isotherm data of Ni(II) onto CHB (initial pH: 7.0; dosage: 1.0 g/L; adsorption time: 6 h; temperature: 25°C).

adsorption (mg/g), K_L (L/mg) is the constant related to the affinity of the adsorbent binding site, K_F ((mg/g)(L/mg)$^{1/n}$) and n are the Freundlich constants related to the adsorption capacity and adsorption intensity, respectively.

Fig. 9 displays the non-linear plots of fitting models. The parameters are calculated and listed in Table 2. It is clear that the adsorption isotherm results can be well described by the Freundlich model. Hence, the adsorption behavior of Ni(II) on CHB suggested a multilayer adsorption.

3.6. Adsorption mechanism of Ni(II) on CHB

To understand the nature of adsorption and identify the possible sites of Ni(II) binding to CHB, FTIR spectra were obtained for CHB before and after Ni(II) adsorption in Fig. 2. After adsorption, the bands of asymmetric and symmetric stretching vibrations of –COO$^-$ groups in CHB shifted from 1,588 and 1,404 cm^{-1} to 1,580 and 1,403 cm^{-1}, respectively, which indicated that carboxyl groups were chelating functional groups for Ni(II). The characteristic band of stretching vibration of O–H and N–H shifted obviously from 3,263 to 3,215 cm^{-1} after adsorption, suggesting that the hydroxyl and amino groups of CHB were involved in Ni(II) adsorption.

To verify the findings from the FTIR spectra, XPS analysis was used to determine the chemical states of the functional groups on the CHB surface before and after Ni(II) adsorption. The O 1s and N 1s XPS spectra are shown in Fig. 10 and the binding energy (BE) data of C 1s, O 1s and N 1s is summarized in Table 3. As shown in Fig. 9 and Table 3, C 1s XPS spectra of CHB showed three characteristics peaks corresponding to C–C and C–H bonds (284.88 eV), C–O bond (286.43 eV) and –COO$^-$ bond (287.93 eV) [35,36]. The XPS spectra of C 1s did not show any noticeable change after Ni(II) adsorption, indicating that these atoms were not involved in the chemical adsorption.

From Fig. 10, the peak at 399.37 eV was contributed to the –NH_2 in the CHB. After adsorption of Ni(II), the peak shifted from 399.37 to 399.91 eV, which indicated the N atoms in the CHB as the electron donor coordinated with Ni(II) [37,38]. Besides, there were two BE peaks in O 1s spectra before adsorption of Ni(II) at 531.35 and 532.66 eV, which were assigned to the oxygen atoms in the C=O groups and C–O, respectively [39,40]. After metal uptake, the peak of C=O weakened while peak of C–O at 532.65 eV remained the same. These results suggest that the oxygen atom in the carboxyl group coordinated with Ni(II) ion to produce the complex. In summary, the XPS results are consistent with the FTIR results.

Table 2
Fitting parameters of the Langmuir and Freundlich

Langmuir			Freundlich		
q_m (mg/g)	K_L	R^2	K_F	n	R^2
124.2	4.938	0.884	100.04	20.8	0.998

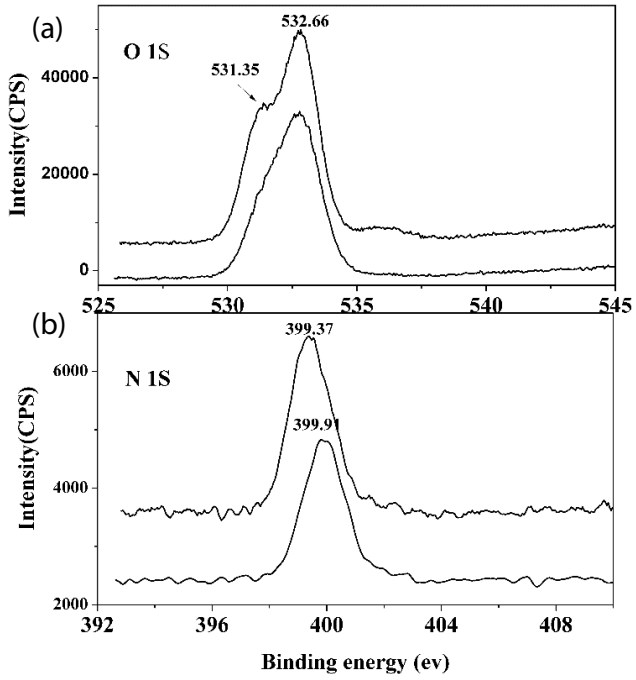

Fig. 10. The O 1s and N 1s XPS spectra of CHB before (a) and after (b) Ni(II) adsorption.

Table 3
BEs of C 1s, O 1s and N 1s on XPS spectra obtained by CHB before and after Ni(II) adsorption

XPS data	C 1s	N 1s	O 1s
CHB	284.88 (C–C, C–H), 286.43	399.37	531.35 (C=O)
	(C–O), 287.93 (COO)	(–NH_2)	532.65 (C–O)
CHB-Ni(II)	284.73 (C–C, C–H), 286.38	399.91	532.65 (C–O)
	(C–O), 287.93(COO)	(–NH_2)	

4. Conclusion

In the present study, cross-linked sodium alginate-carboxymethyl chitosan hydrogel (CHB) was prepared and characterized with FTIR, SEM and EDS. The adsorption parameters were evaluated by using the batch adsorption method, and adsorption equilibrium was obtained in 6 h at pH 7.0 with adsorption capacity of 128.4 mg/g. The kinetics of the experimental data were fitted with the pseudo-second-order model and the Freundlich model fit the adsorption data better. Adsorption–desorption studies showed that CHB was completely regenerated up to five cycles using 0.01 M HCl. In summary, a low-cost CHB exhibited good adsorption ability and good regeneration ability. Thus, the blended hydrogels are potentially to be used for the removal of Ni(II) from the wastewater.

Acknowledgements

This work was financially supported by the Anhui Provincial Key Research and Development Project (2022h11020005).

References

[1] E. Repo, J.K. Warchol, T.A. Kurniawan, M.E. Sillanpää, Adsorption of Co(II) and Ni(II) by EDTA-and/or DTPA-modified chitosan: kinetic and equilibrium modeling, Chem. Eng. J., 161 (2010) 73–82.
[2] A.H. Shalla, Z. Yaseen, M.A. Bhat, T.A. Rangreez, M. Maswal, Recent review for removal of metal ions by hydrogels, Sep. Sci. Technol., 54 (2019) 89–100.
[3] H. Masoumi, A. Ghaemi, H.G. Gilani, Evaluation of hypercross-linked polymers performances in the removal of hazardous heavy metal ions: a review, Sep. Purif. Technol., 260 (2021) 118221, doi: 0.1016/j.seppur.2020.118221.
[4] M. Agarwal, K. Singh, Heavy metal removal from wastewater using various adsorbents: a review, J. Water Reuse Desal., 7 (2017) 387–419.
[5] A. Shafique, Removal of toxic pollutants from aqueous medium through adsorption: a review, Desal. Water Treat., 234 (2021) 38–57.
[6] S. Martini, S. Afroze, K.A. Roni, M. Setiawati, D. Kharismadewi, A review of fruit waste-derived sorbents for dyes and metals removal from contaminated water and wastewater, Desal. Water Treat., 235 (2021) 300–323.
[7] Z. Al-Qodah, M.A. Yahya, M. Al-Shannag, On the performance of bioadsorption processes for heavy metal ions removal by low-cost agricultural and natural by-products bioadsorbent: a review, Desal. Water Treat., 85 (2017) 339–357.
[8] M. Nasrollahzadeh, M. Sajjadi, S. Iravani, R.S. Varma, Starch, cellulose, pectin, gum, alginate, chitin and chitosan derived (nano) materials for sustainable water treatment: a review, Carbohydr. Polym., 251 (2021) 116986, doi: 10.1016/j.carbpol.2020.116986.
[9] J. Kaur, P. Sengupta, S. Mukhopadhyay, Critical review of bioadsorption on modified cellulose and removal of divalent heavy metals (Cd, Pb, and Cu), Ind. Eng. Chem. Res., 61 (2022) 1921–1954.
[10] Z.A. Sutirman, M.M. Sanagi, W.I.W. Aini, Alginate-based adsorbents for removal of metal ions and radionuclides from aqueous solutions: a review, Int. J. Biol. Macromol., 174 (2021) 216–228.
[11] H.B. Quesada, T.P. de Araújo, D.T. Vareschini, M.A.S.D. de Barros, R.G. Gomes, R. Bergamasco, Chitosan, alginate and other macromolecules as activated carbon immobilizing agents: a review on composite adsorbents for the removal of water contaminants, Int. J. Biol. Macromol., 164 (2020) 2535–2549.
[12] H. Musarurwa, N.T. Tavengwa, Application of carboxymethyl polysaccharides as bio-sorbents for the sequestration of heavy metals in aquatic environments, Carbohydr. Polym., 237 (2020) 116142, doi: 10.1016/j.carbpol.2020.116142.
[13] H. Javadian, M. Ruiz, T.A. Saleh, A.M. Sastre, Ca-alginate/carboxymethyl chitosan/$Ni_{0.2}Zn_{0.2}Fe_{2.6}O_4$ magnetic bionanocomposite: synthesis, characterization and application for single adsorption of Nd^{+3}, Tb^{+3}, and Dy^{+3} rare earth elements from aqueous media, J. Mol. Liq., 306 (2020) 112760, doi: 10.1016/j.molliq.2020.112760.
[14] Q. Song, J. Gao, Y. Lin, Z. Zhang, Y. Xiang, Synthesis of cross-linking chitosan-PVA composite hydrogel and adsorption of Cu(II) ions, Water Sci. Technol., 81 (2020) 1063–1070.
[15] X. Gao, C. Guo, J. Hao, Z. Zhao, H. Long, M. Li, Adsorption of heavy metal ions by sodium alginate-based adsorbent-a review and new perspectives, Int. J. Biol. Macromol., 164 (2020) 4423–4434.
[16] H. Wang, Y. Wang, C. Li, L. Jia, Fabrication of eco-friendly calcium cross-linked alginate electrospun nanofibres for rapid and efficient removal of Cu(II), Int. J. Biol. Macromol., 219 (2022) 1–10.
[17] Y. Na, J. Lee, S.H. Lee, P. Kumar, J.H. Kim, R. Patel, Removal of heavy metals by polysaccharide: a review, Polym. Plast. Technol. Mater., 59 (2020) 1770–1790.
[18] P.M. Pakdel, S.J. Peighambardoust, Review on recent progress in chitosan-based hydrogels for wastewater treatment application, Carbohydr. Polym., 201 (2018) 264–279.
[19] H. Shehzad, E. Ahmed, A. Sharif, Z.H. Farooqi, M.I. Din, R. Begum, I. Nawaz, Modified alginate-chitosan-TiO_2 composites for adsorptive removal of Ni(II) ions from aqueous medium, Int. J. Biol. Macromol., 194 (2022) 117–127.
[20] S. Potiwiput, H. Tan, G. Yuan, S. Li, T. Zhou, J. Li, Y. Chen, Dual-cross-linked alginate/carboxymethyl chitosan hydrogel containing in situ synthesized calcium phosphate particles for drug delivery application, Mater. Chem. Phys., 241 (2020) 122354, doi: 10.1016/j.matchemphys.2019.122354.
[21] X.G. Chen, H.J. Park, Chemical characteristics of O-carboxymethyl chitosans related to the preparation conditions, Carbohydr. Polym., 53 (2003) 355–359.
[22] X. Wang, H. Zhang, Q. He, H. Xing, K. Feng, F. Guo, W. Wang, Core-shell alginate beads as green reactor to synthesize grafted composite beads to efficiently boost single/co-adsorption of dyes and Pb(II), Int. J. Biol. Macromol., 206 (2022) 10–20.
[23] R. Benaddi, F. Aziz, H.K. El, N. Ouazzani, Adsorption and desorption studies of phenolic compounds on hydroxyapatite-sodium alginate composite, Desal. Water Treat., 220 (2021) 297–308.
[24] W. Luo, Z. Bai, Y. Zhu, Comparison of Co(II) adsorption by a cross-linked carboxymethyl chitosan hydrogel and resin: behaviour and mechanism, New J. Chem., 41 (2017) 3487–3497.
[25] C.X. Wang, Q.P. Song, Removal of Cu(II) ions from aqueous solutions using N-carboxymethyl chitosan, Water Sci. Technol., 66 (2012) 2027–2032.
[26] W. Wang, Q. Lu, Z. Zhuo, W. Zhang, H. Liu, J. Zhang, T. Guerrero, Synthesis and characterization of recyclable O-carboxymethyl chitosan Schiff base for the effective removal of Cd(II) from aqueous solution, Desal. Water Treat., 189 (2020) 264–275.
[27] Y. Song, N. Wang, L.Y. Yang, Y.G. Wang, D. Yu, X.K. Ouyang, Facile fabrication of ZIF-8/calcium alginate microparticles for highly efficient adsorption of Pb(II) from aqueous solutions, Ind. Eng. Chem. Res., 58 (2019) 6394–6401.
[28] M. Hassan, R. Naidu, J. Du, F. Qi, M.A. Ahsan, Y. Liu, Magnetic responsive mesoporous alginate/β-cyclodextrin polymer beads enhance selectivity and adsorption of heavy metal ions, Int. J. Biol. Macromol., 207 (2022) 826–840.
[29] Y. Zhang, S. Lin, J. Qiao, D. Kołodyńska, Y. Ju, M. Zhang, D.D. Dionysiou, Malic acid-enhanced chitosan hydrogel beads (mCHBs) for the removal of Cr(VI) and Cu(II) from aqueous solution, Chem. Eng. J., 353 (2018) 225–236.
[30] E.I. Ugwu, A. Othmani, C.C. Nnaji, A review on zeolites as cost-effective adsorbents for removal of heavy metals from aqueous environment, Int. J. Environ. Sci. Technol., 19 (2022) 8061–8084.

[31] R.J. Kongarapu, A.K. Nayak, M.U. Khobragade, A. Pal, Surfactant bilayer on chitosan bead surface for enhanced Ni(II) adsorption, Sustain. Mater. Technol., 18 (2018) e00077, doi: 10.1016/j.susmat.2018.e00077.
[32] P. Yu, H.Q. Wang, R.Y. Bao, Z. Liu, W. Yang, B.H. Xie, M.B. Yang, Self-assembled sponge-like chitosan/reduced graphene oxide/montmorillonite composite hydrogels without cross-linking of chitosan for effective Cr(VI) sorption, ACS Sustainable Chem. Eng., 5 (2017) 1557–1566.
[33] M.J. Ahmed, B.H. Hameed, Insights into the isotherm and kinetic models for the co-adsorption of pharmaceuticals in the absence and presence of metal ions: a review, J. Environ. Manage., 252 (2019) 109617, doi: 10.1016/j.jenvman.2019.109617.
[34] T. Hu, Q. Liu, T. Gao, K. Dong, G. Wei, J. Yao, Facile preparation of tannic acid–poly(vinyl alcohol)/sodium alginate hydrogel beads for methylene blue removal from simulated solution, ACS Omega, 3 (2018) 7523–7531.
[35] T. Huang, Y.W. Shao, Q. Zhang, Y.F. Deng, Z.X. Liang, F.Z. Guo, Y. Wang, Chitosan-cross-linked graphene oxide/carboxymethyl cellulose aerogel globules with high structure stability in liquid and extremely high adsorption ability, ACS Sustainable Chem. Eng., 7 (2019) 8775–8788.
[36] J. Yuan, C. Yi, H. Jiang, F. Liu, G.J. Cheng, Direct ink writing of hierarchically porous cellulose/alginate monolithic hydrogel as a highly effective adsorbent for environmental applications, ACS Appl. Polym. Mater., 3 (2021) 699–709.
[37] W. Luo, Z. Bai, Y. Zhu, Fast removal of Co(II) from aqueous solution using porous carboxymethyl chitosan beads and its adsorption mechanism, RSC Adv., 8 (2018) 13370–13387.
[38] P. Zhang, K. Zou, L. Yuan, J. Liu, B. Liu, T.P. Qing, B. Feng, A biomass resource strategy for alginate-polyvinyl alcohol double network hydrogels and their adsorption to heavy metals, Sep. Purif. Technol., 301 (2022) 122050, doi: 10.1016/j.seppur.2022.122050.
[39] H. Luo, Y. Liu, H. Lu, Q. Fang, H. Rong, Efficient adsorption of tetracycline from aqueous solutions by modified alginate beads after the removal of Cu(II) ions, ACS Omega, 6 (2021) 6240–6251.
[40] Q. Liao, H. Rong, M. Zhao, H. Luo, Z. Chu, R. Wang, Strong adsorption properties and mechanism of action with regard to tetracycline adsorption of double-network polyvinyl alcohol-copper alginate gel beads, J. Hazard. Mater., 4229 (2022) 126863, doi: 10.1016/j.jhazmat.2021.126863.